



# **Applicability of Self-Powered Synchronized Electric Charge Extraction (SECE) Circuit for Piezoelectric Energy Harvesting**

**Action Nechibvute<sup>1</sup>, Pearson Luhanga<sup>1</sup> Albert Chawanda<sup>1</sup>**

<sup>1</sup>Department of Applied Physics & Telecommunications, Midlands State University, P/Bag 9055, Gweru, Zimbabwe

<sup>2</sup>Physics Department, University of Botswana, P/Bag 0022, Gaborone, Botswana

## **ABSTRACT**

In recent years, nonlinear techniques have been proposed to enhance the energy harvested capabilities of piezoelectric generators. Among these techniques, synchronous electric charge extraction (SECE) has been one that has been investigated. The SECE technique is principally a power conversion process that harvests electrical energy when charge accumulated on the intrinsic capacitance of the piezoelectric material reaches a maximum. In this work, we present the results of experimental investigations of the performance of a self-powered SECE interface circuit designed around the self-powered electronic breaker which employs PNP and NPN transistors for switching. The experimental results show that for the piezoelectric bimorph transducer used, the self-powered SECE circuit can harvest up to about 70 % more power compared to the standard energy harvesting (SEH) interface circuit.

**Keywords:** *Synchronised electric charge extraction, energy harvesting, Interface circuit, piezoelectric, self-powered*

## **1. INTRODUCTION**

Nonlinear switching techniques have attracted a lot of interest as a means of enhancing the energy harvesting capabilities of piezoelectric devices [1-4]. Among these nonlinear techniques, synchronized electric charge extraction (SECE) has been pursued as one of the most promising techniques. In reported literature, the study of the SECE technique is mainly done based on externally powered switching units and in some cases only limited to theoretical and simulation studies [5-8]. While the applicability of the SECE technique is theoretical plausible with a possibility of increasing the energy harvested by the standard energy harvesting (SEH) interface by up to four times, the practical realization of the SECE interface circuit is fairly challenging [9-11].

Firstly, unlike the externally powered interfaces, a practically viable SECE interface circuit must of necessity be self-powered. Secondly, the switching elements of the self-powered circuit should dissipate very little energy harvested by piezoelectric transducer. The self-powered electronic breaker suggested by Richard [12] is an appealing circuit since it can dissipate very little power (about 5 % of the harvested power) while at the same time it meets the timing requirements demanded by the synchronized switching design.

Despite some reported works on SECE interface circuits, there is still a lot of experimental investigations which need to be done to understand the performance of self-powered nonlinear circuits [13-16].

The performance of self-powered synchronized energy harvesting interfaces is seldom reported as a function of the vibration excitation level. In fact, the enhancement offered by an

ideal SECE interface circuit over the SEH interface circuit is taken to be constant, i.e. independent of the excitation level. This assumption is not adequately validated by experimental work based on self-powered nonlinear interfaces.

In this paper, the performance of a self-powered SECE interface circuit based on the electronic breaker circuit is studied under different vibration excitation levels. The applicability of the circuit for both resonant and off-resonant conditions is presented and comparisons are made relative to the standard energy harvesting (SEH) interface. Section 2 presents a brief overview of SECE technique. Section 3 presents the experimental setup and procedures, and experimental results and discussion. Finally, section 4 concludes the paper.

## **2. THE SECE CIRCUIT AND PRINCIPLE**

The SECE technique involves the extraction of all the electric charge on the piezoelectric transducer periodically and transferring the corresponding amount of electric energy to the circuit load. The SECE technique involves the extraction of all the electric charge on the piezoelectric transducer periodically and transferring the corresponding amount of electric energy to the circuit load. Fig. 1 shows the basic SECE circuit schematic. The switch is always open during the resonance period except at the short time instances when the vibration displacement of the energy harvesting beam structure reaches its peak amplitude. Thus, with the switch open electric charge accumulates on the piezoelectric capacitance,  $C_p$ . When the displacement of the structure comes at its maximum, the voltage is maximized and the switch is closed for a short time, allowing for electrical energy accumulated on  $C_p$  to be transferred to the storage capacitor  $C_s$  and the load. The typical waveforms are shown in Fig. 2. For the maximum displacement given by  $u_m$ , and

piezoelectric coupling parameter  $\theta$ , the average power harvested by the SECE interface is given by Eq. (1):

$$P = \frac{2\omega\theta^2 u_m^2}{\pi C_p} \quad (1)$$

From Eq.(1), it is apparent that the energy harvested using an ideal SECE interface is independent of the load.

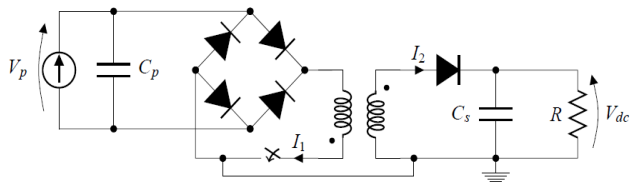


Figure 1: SECE circuit schematic

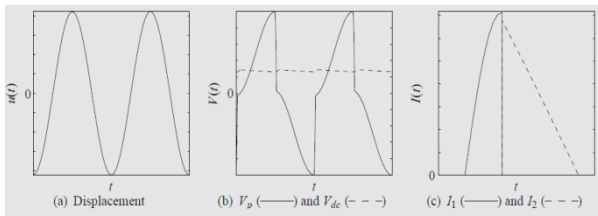


Figure 2: SECE typical theoretical waveforms

The self-powered SECE interface circuit considered in this study was initially proposed and theoretically analysed by Zhu et al [17] and is shown in Fig. 3. As noted earlier, the piezoelectric element is in open circuit phase most of the time. In this phase, transistors  $T_1$  and  $T_2$  in the electronic breaker circuit blocked and hence are non-conducting.

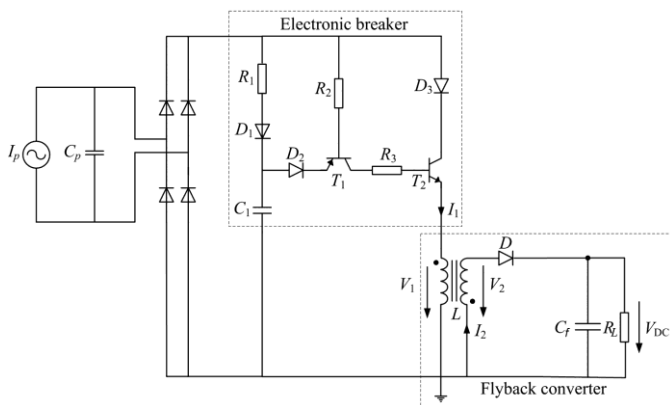


Figure 3: Self-powered SECE interface circuit [17]

When the peak displacement of the vibrating structure is reached, the transistors  $T_1$  and  $T_2$  are now in conducting mode, and results in the charge accumulated on piezoelectric capacitance  $C_p$  being

transferred into the inductor  $L$  through  $D_3$  and  $T_2$ . The energy transfer process is completed when the current through the primary winding of the Flyback transformer reaches its maximum value and the voltage across the transformer drops to zero. Unlike the standard transformer whose only function is to coupling energy from the primary to the secondary windings, the flyback transformer also functions to store energy within the air gap.

### 3. EXPERIMENTAL STUDIES

#### 3.1 Experimental Setup and Procedures

A geometrically optimized piezoelectric series bimorph device with a proof mass was used as the energy harvesting transducer. The device was fabricated using two PSI-5H4E ceramic patches with nickel-plated electrodes (Piezo Systems Inc, USA) bonded to a stainless steel using conducting epoxy glue (Circuit Works, USA). The piezoelectric patches were electrically connected in series. The total device volume is about  $5.5 \text{ mm}^3$ . Table 1 gives the dimensions of the piezoelectric bimorph beam. To implement the self-powered circuit in Fig. 3, the electronic components with values shown in Table 2 were used.

The piezoelectric bimorph device was clamped to an electromagnetic shaker, and the shaker was driven by a sinusoidal excitation signal which was generated by a function generator (Universal Test System MS9150-Metex Instruments). The ADXL202 accelerometer (Analogue Devices, USA), which has a typical sensitivity of  $312 \text{ mV/g}$  when operating from a  $5 \text{ V}$  power supply, was fixed at the clamped end to measure acceleration. The bimorph device was driven at its first-mode natural frequency of  $49.87 \text{ Hz}$ .

Table 1: Dimensions of the Piezoelectric Device

	<i>Dimensions (Thickness x Width x thickness)</i>
Substrate (Stainless Steel)	0.120 mm x 4.0 mm x 28.25mm
Piezoelectric material (PSI-5H4E )	0.127 mm x 4.0 mm x 9.41 mm
Proof mass-(lead metal)	7.000 mm x 4.0 mm x 18.83 mm

Table 2: Components for self-powered SECE

<i>Component</i>	<i>Specification/Value</i>
Transistors	$T_1$ & $T_3$ (PNP) -BD 140 $T_2$ & $T_4$ (NPN) -BD139

Capacitors	C <sub>1</sub> -330 pF C <sub>r</sub> - 1μF
Flyback transformer	L -6 mH
Resistors	R <sub>1</sub> -180 kΩ R <sub>2</sub> & R <sub>3</sub> -3.3 kΩ
Diodes	D <sub>1</sub> , D <sub>2</sub> & D <sub>3</sub> -IN4004

With the piezoelectric transducer device driven at resonance, the output was first connected to the SEH interface. The output load resistance R<sub>L</sub> was varied and the voltage across the resistance was measured using a digital multimeter (true rms DMM, Fluke). This procedure was repeated for the following values of excitation acceleration levels: 0.1 g, 0.2 g, 0.3 g, 0.4 g, and 0.5 g. The excitation level beyond 0.5 g amplitude was avoided to eliminate the possibility of exceeding the displacement limits and damaging the piezoelectric transducer device. Using the same test conditions, the self-powered SSHI was then connected in place of the SEH. The accelerometer output signal and the output voltage signals from the interfaces were monitored by a digital storage oscilloscope (ISOTECH-IDS-8062). The results of the experimental study are presented in Section 3.2.

### 3.2 Experimental Results and Discussion

Fig. 4 shows the oscilloscope trace of the voltage output waveform from the self-powered SECE interface circuit. The waveform compares very well with the expected theoretical waveform shown in Fig 2.

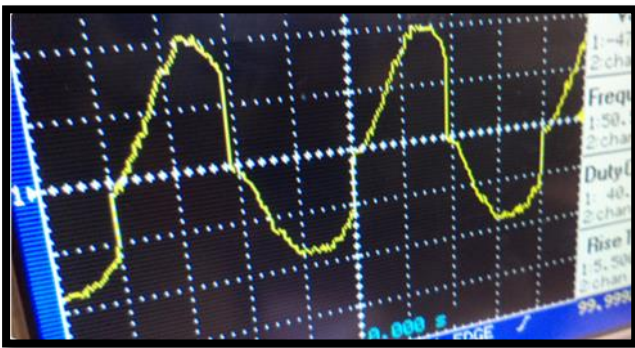


Figure 4: CRO screenshot showing the self-powered SECE output voltage

The resonance performance (at excitation frequency of about 50 Hz) of the SEH and self-powered SECE interfaces is shown in Figs. 5 and 6, respectively. Comparing Figs 5 and 6 shows that the SEH interface delivers optimum power at an optimum resistance of 1 MΩ while the SECE interface shows that optimum power is fairly independent of the load resistances.

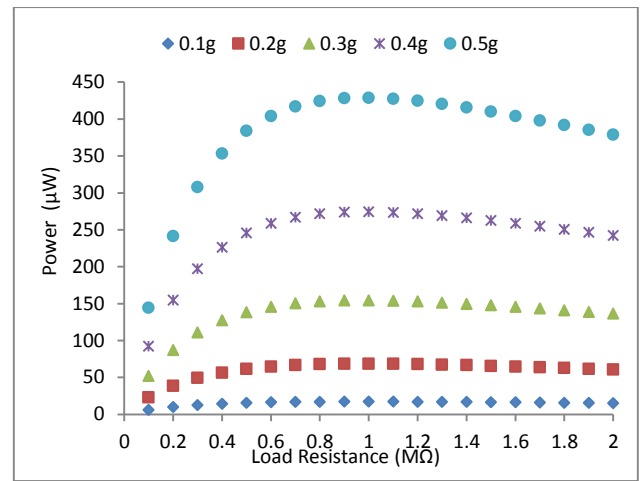


Figure 5: Power output of SEH interface circuit for different excitation levels

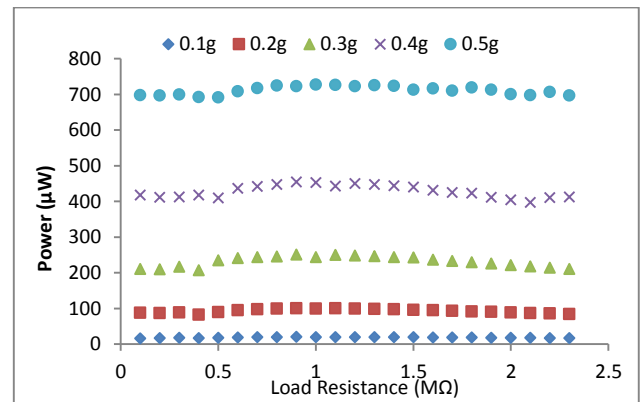


Figure 6: Power output of self-powered SECE interface circuit for different excitation levels

Table 3 summarises the extent of enhancement of the self-powered SECE interface relative to the SEH interface. Results in Table 3 show that an increase in input acceleration will result in an increased performance enhancement by the self-powered SECE interface. This is unlike the ideal SECE which has a constant gain over the SEH for different excitation levels.

Table 3: Extent of enhancement as a function of excitation level (at resonance)

Excitation level (g)	Optimum power (μW)		$\beta = P_{SECE}/P_{SEH}$
	SEH	SECE	
0.1	17.13	20.523	1.198
0.2	68.53	100.57	1.468
0.3	154.36	251.17	1.627
0.4	274.42	455.06	1.658

0.5	428.755	728.01	1.698
-----	---------	--------	-------

In the experimental investigations, the vibration frequency of 38 Hz (or normalised frequency of  $\Omega = 0.76$ ) was observed to result in the dramatic decrease in the voltage response of the piezoelectric transducer, and was therefore taken to represent the ‘off-resonance’ condition. Fig 7 and Table 4 compare the off-resonance and resonance performance at excitation level of 0.5 g.

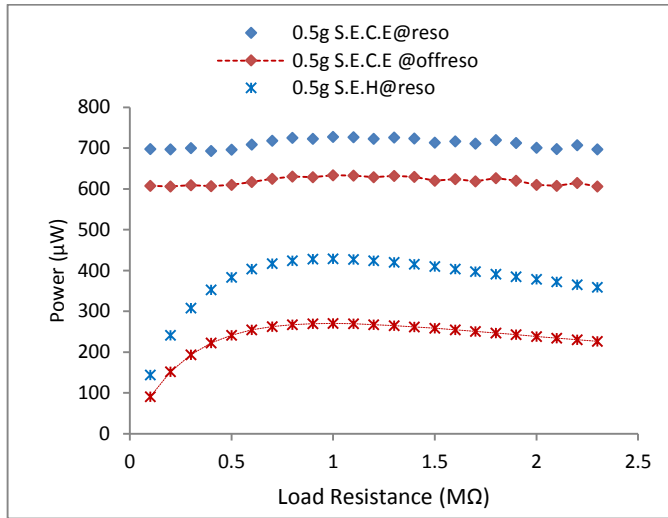


Figure 7: Comparison of resonance and off resonance performance at 0.5 g.

Table 4: Resonance versus off-resonance performance (at 0.5 g excitation).

	Power (µW)		$\beta = P_{SECE}/P_{SEH}$
	SEH	SECE	
At resonance	428.755	728.01	1.698
Off-resonance	270.116	633.36	2.34477

Under acceleration amplitude of 0.5 g, the SEH delivered an optimum power of 428.755 µW while the self-powered SSHI interface delivered an optimum power of 728.01 µW when operating at resonance. This suggests that the self-powered SECE has a gain of the order of 70 % for input acceleration beyond 0.5 g. Under off resonance conditions (with  $\Omega = 0.76$ ) and an acceleration of 0.5 g, SEH delivered an optimum power of 270.12 µW while the self-powered SSHI interface delivered an output power of 633.36 µW. Thus the self-powered SECE interface circuit has a power increase of 134 % over the SEH interface under off resonance operation. This is an interesting

result because it suggests that the SECE interface circuit can be employed to increase the frequency bandwidth of energy harvesting systems

#### 4. CONCLUSIONS

In this paper, the performance of a self-powered SECE interface circuit to enhance the energy harvesting capabilities of a piezoelectric bimorph device was presented. The experimental results show that for the piezoelectric bimorph transducer used, the self-powered SECE circuit can harvest up to about 70 % more power compared to the standard energy harvesting (SEH) interface circuit. As the input acceleration increases, the enhancement of the self-powered SECE over the SEH interface becomes very significant. This is unlike the ideal SECE which has a constant gain over the SEH for various excitations (and predicted enhancement of four times the power generated by the SEH interface). While the self-powered SECE circuit has shown significant gains over the SEH interface, the predictions of the ideal SECE are not consistent with the experimental results of the self-powered interface. Consequently, there still exist design challenges that need to be further investigated to accurately model and predict the performance of self-powered SECE interfaces.

#### REFERENCES

- [1] Badel, A., Guyomar, D., Lefeuvre, E., & Richard, C. (2006). Piezoelectric energy harvesting using a synchronized switch technique. *Journal of Intelligent Material Systems and Structures*, 17(8-9), 831-839.
- [2] Guyomar, D., Badel, A., Lefeuvre, E., & Richard, C. (2005). Toward energy harvesting using active materials and conversion improvement by nonlinear processing. *Ultrasonics, Ferroelectrics and Frequency Control, IEEE Transactions on*, 52(4), 584-595.
- [3] Lefeuvre, E., Badel, A., Richard, C., & Guyomar, D. (2005). Piezoelectric energy harvesting device optimization by synchronous electric charge extraction. *Journal of Intelligent Material Systems and Structures*, 16(10), 865-876.
- [4] Lallart, M., & Guyomar, D. (2008). An optimized self-powered switching circuit for non-linear energy harvesting with low voltage output. *Smart Materials and Structures*, 17(3), 035030.
- [5] Arroyo, E., & Badel, A. (2011). Electromagnetic vibration energy harvesting device optimization by synchronous energy extraction. *Sensors and Actuators A: Physical*, 171(2), 266-273.

- [6] Wang, Y. (2012). *Simultaneous Energy Harvesting and Vibration Control via Piezoelectric Materials* (Doctoral dissertation, Virginia Polytechnic Institute and State University).
- [7] Wickenheiser, A. M., Reissman, T., Wu, W. J., & Garcia, E. (2010). Modeling the effects of electromechanical coupling on energy storage through piezoelectric energy harvesting. *Mechatronics, IEEE/ASME Transactions on*, 15(3), 400-411.
- [8] Lefeuvre, E., Badel, A., Richard, C., & Guyomar, D. (2005). Piezoelectric energy harvesting device optimization by synchronous electric charge extraction. *Journal of Intelligent Material Systems and Structures*, 16(10), 865-876.
- [9] Tang, L., & Yang, Y. (2011). Analysis of synchronized charge extraction for piezoelectric energy harvesting. *Smart Materials and Structures*, 20(8), 085022.
- [10] Lefeuvre, E., Badel, A., Richard, C., Petit, L., & Guyomar, D. (2006). A comparison between several vibration-powered piezoelectric generators for standalone systems. *Sensors and Actuators A: Physical*, 126(2), 405-416.
- [11] Schlichting, A. D., Phadke, A., & Garcia, E. (2013, April). Practical implementation of piezoelectric energy harvesting synchronized switching schemes. In *SPIE Smart Structures and Materials+ Nondestructive Evaluation and Health Monitoring* (pp. 86880A-86880A). International Society for Optics and Photonics.
- [12] Richard, C., Guyomar, D., & Lefeuvre, E. (2007). Self-powered electronic breaker with automatic switching by detecting maxima or minima of potential difference between its power electrodes. *FR2005/003000, publication number: WO/2007/063194*.
- [13] Wu, Y., Badel, A., Formosa, F., Liu, W., & Agbossou, A. (2013). Two self-powered energy harvesting interfaces based on the optimized synchronous electric charge extraction technique. In *Journal of Physics: Conference Series* (Vol. 476, No. 1, pp. 12098-12102). IOP Publishing.
- [14] Liu, W. Q., Badel, A., Formosa, F., Wu, Y. P., & Agbossou, A. (2013). Wideband energy harvesting using a combination of an optimized synchronous electric charge extraction circuit and a bistable harvester. *Smart Materials and Structures*, 22(12), 125038.
- [15] Wu, Y., Badel, A., Formosa, F., Liu, W., & Agbossou, A. (2014). Self-powered optimized synchronous electric charge extraction circuit for piezoelectric energy harvesting. *Journal of Intelligent Material Systems and Structures*, 1045389X13517315.
- [16] Zhao, L., Tang, L., Wu, H., & Yang, Y. (2014, March). Synchronized charge extraction for aeroelastic energy harvesting. In *SPIE Smart Structures and Materials+ Nondestructive Evaluation and Health Monitoring* (pp. 90570N-90570N). International Society for Optics and Photonics.
- [17] Zhu, L., Chen, R., & Liu, X. (2012). Theoretical analyses of the electronic breaker switching method for nonlinear energy harvesting interfaces. *Journal of Intelligent Material Systems and Structures*, 23(4), 441-451.